

***FLOW-3D*[®] PREDICTIONS FOR FREE DISCHARGE AND SUBMERGED PARSHALL FLUMES**

C.W. Hirt and K.A. Williams
Flow Science, Inc.
July 25, 1994

INTRODUCTION

Open channel hydraulic systems often use Parshall flumes to measure the rate of flow in the system. The Parshall flume has a special shape that is designed to facilitate flow measurements while mostly eliminating the problem of sediment deposition that could lead to an incorrect measurement. Flumes are preferable to weirs because they typically have only about 25% of the head loss associated with a weir.

The above properties of Parshall flumes were derived from a manual kindly sent to the authors by Mr. Jim Higgs of the Bureau of Reclamation in Denver, Colorado. The manual contains a detailed discussion and extensive tables for the design and use of Parshall flumes. We shall refer to this manual as WMM, which stands for "Water Measurement Manual," U.S. Dept. Interior, Denver, CO, revised reprint 1984.

Parshall flumes come in sizes that range from inches to many feet. In this study we concentrate on a one foot flume and demonstrate how *FLOW-3D* can be used to model the full range of operating conditions from free discharge to nearly complete submergence.

The concept of free discharge versus submerged flow can be understood by considering a fixed headwater height and asking what happens as the tailwater level is changed. If the tailwater level is the same as that of the headwater, there will be no flow. As the tailwater level is slowly reduced, flow through the flume will increase but only up to a limiting value. Once the limiting, free-flow value is reached, further reduction in the tailwater level produces no further increase in the flow rate.

DESCRIPTION OF COMPUTATIONAL MODEL

Flow Science's commercial computational fluid dynamics (CFD) software package *FLOW-3D*[®] was used to predict flow behavior in a one foot Parshall flume under both free discharge and large submergence operation. This section describes the *FLOW-3D* physical model setup, boundary and initial conditions, and fluid physics model selections.

The basic Parshall flume has a converging entrance section, followed by a narrow throat section and then a diverging section for discharge. The entrance has a horizontal bed, called the crest, that is slightly elevated with respect to the bed in the headwater region. In the throat section the bed slopes down, while in the diverging section the bed slopes upward.

In our computational model we have followed the recommended dimensions for a one foot flume given in WMM (Fig. 19), here reproduced as Fig. 1a. A 1.25 foot long converging section, preceded by a 0.75 foot section of the headwater channel, was placed upstream of the entrance to the flume. At the flume exit we placed a similar 1.25 foot diverging section and a 0.75 foot section of the tailwater channel. The headwater and tailwater channels are assumed to have a width of 4.896 feet. Because of transverse symmetry, we have chosen to model only one half of the flume.

The *FLOW-3D* geometry model was generated so that it could be easily extended to a full flume (i.e., both symmetric halves) should we later be interested in investigating, for example, the influence of non-symmetric or non-uniform headwater conditions.

For the free discharge case a computational grid covering the region to be modeled consisted of 80 mesh cells in the streamwise direction, 14 cells in the transverse direction and 18 cells vertically. With boundary cells the total cell number was 26,880 cells. An initial calculation used 14 cells in the vertical direction and gave results very close to the more refined case reported in this note. For the submerged cases, 16 to 20 cells were used in the vertical direction.

The geometry of the flume and its connections to the upstream and downstream channels was modeled using two obstacles consisting of ten functions that describe subregions bounded by plane surfaces.

Boundary conditions for the fluid consisted of specifying the fluid heights (and hydrostatic pressures) at the inlet and outlet. When flow enters the computational region, we assume it does so starting from rest, which is a good approximation to having a large reservoir upstream.

Initial conditions were simplified by assuming the fluid to be at rest and that the fluid level upstream of the entrance to the flume's throat was at the headwater height while fluid downstream of the throat entrance was at the same height as the tailwater. This prescription leads to a discontinuity in the free surface elevation, but it does not cause any computational difficulties.

For all the computations reported in this note the headwater level was 0.8 feet above the crest (or 1.05 feet above the channel bed).

The standard density and viscosity of water were used for all calculations. Because this type of flow is expected to be dominated by inertia and gravitational effects, with viscous effects exerting a very small influence on the flow, we did not include wall shear stresses. We did, however, include a turbulence model because we expected turbulence to develop in localized regions such as hydraulic jumps.

There are several possibilities for turbulence models and very little data to support the selection of one over another for the present application. To satisfy our intuition that the most important feature of turbulence is the smoothing or mixing of fluid in the vicinity of strong velocity shears (e.g., hydraulic jumps and flow separations) we elected to use the Large Eddy Simulation (LES) model. This model generates a turbulent viscosity proportional to the local rate of strain in the fluid, so it has the basic property expected by intuition. Strictly speaking, however, accurate application of the LES model requires a much finer mesh that captures all the important energy containing eddies in the flow, and it should have some stochastic feature at the inflow boundary to seed the turbulence. Nevertheless, we shall use this model with a modest value for the LES coefficient of 0.1 (the default in *FLOW-3D*).

Flow rates through Parshall flumes are computed from two measurements of stagnation pressures at locations H_a and H_b indicated in Fig. 1a. We have located history data recorders at these locations in the computations.

The complete input file for the free discharge case is given in Fig. 2 and includes all grid, geometric and boundary condition data plus all physical and computational parameters. This short input file is typical for *FLOW-3D*. Pictures of the grid, geometry and initial fluid configuration are shown in Fig. 1b-d.

FREE DISCHARGE PARSHALL FLUME

The first case we consider has a tailwater height of 0.25 feet above the flume crest, which is sufficiently below the headwater (0.8 feet above the crest) to produce free discharge conditions.

A calculation was performed that followed the initial transient out to a time of 11.77 s. At this time the inlet flow rate and the pressure at the Parshall flume measuring location H_a were steady with much less than 1% variations, see Fig. 3. Some unsteadiness persists in the tailwater flow rate (about 2.9%) and at the pressure measuring location H_b because of wave reflections at the outlet boundary. These reflections might be reduced by including a larger portion of the tailwater region in the computations.

The CPU time for this computation was approximately 6.33 hours on an IBM 6000/320 workstation. With a slightly coarser mesh virtually the same results were obtained in about 4.5 hours of CPU time. Newer, low level workstations should be able to complete the fine mesh computations in about 1 to 3 hours, and a 486/66 PC would take on the order of 10 hours.

Flow configurations and velocity distributions at the completion of the calculation are shown in Fig. 4. We see that the flow passing over the crest and across the sloping bed of the diverging section of the flume is very smooth, Fig. 4a. Just downstream of the flume's exit the flow exhibits a hydraulic jump, Figs. 4a and 4b, that slows the flow and raises its elevation. There is a three-dimensional velocity profile at the outlet in which the center of the flow leaving the flume has a higher velocity, Fig. 4c.

The expected flow rate under free-flow conditions is, according to Table 16 in WMM, equal to 2.85 cfs. When using Table 16, one is instructed to use the stagnation pressure (or head) at location H_a . If there are no losses, this value should equal the head at stagnation conditions in the headwater region. In our model this is the head at the inlet boundary, 0.8 feet because we used a stagnation condition at the inlet, PBCTYP=1.0.

The calculated pressure at location H_a is 0.696 ft, which is a static pressure and must be corrected for the dynamic head. This pressure is also at the center of a computational mesh cell and must be increased by the hydrostatic pressure equivalent to one half cell height to correspond to the head above the flume crest. Making these corrections, we find that the total head is very close to the specified inlet head at location H_a of 0.8 feet.

The computed volume flow rate entering the flume is 2.72 cfs, which is 4.6% below the lower computed flow rate value we used, and the surface height difference is less than one third of the minimum cell size used to resolve surface variations.

It should be kept in mind that the reported value in WMM comes from an empirical correlation and contains some measure of approximation. For example, in a memorandum report prepared by Hilaire Peck of the U.S. Bureau of Reclamation, "Submerged Flow in Parshall Flumes," PAP-523, April 1988, the measured flow rate in the one foot Parshall flume located at the Bureau is well correlated with the expression,

$$Q = 3.95 H_a^{1.55} \text{ (Equ.1 of Peck Ref.)}$$

Using this formula, the flow rate for a 0.8 foot head is 2.795 cfs, which is only 2.68% larger than our computations. Since this data is more recent than that presented in WMM, we believe it to be more accurate.

Aside from numerical resolution errors, one possible reason for the remaining small difference in computed and empirical flow rates is the limited entrance region included in the

computational model. The empirical flow rate is based on the head in the incoming stream upstream of the flume entrance. In our model a very small upstream region was modeled, and we see a definite flow structure develop over the inlet surface. This suggests that a larger entrance region should be investigated in future studies.

In any case, considering the numerical resolution and the limited upstream region included in the model, our computations are remarkably close (2.68%) to measured flow rates.

MODERATELY SUBMERGED PARSHALL FLUME

To illustrate the capabilities of *FLOW-3D* for treating submerged conditions, we have chosen a tailwater height of 0.68 feet, which is 85% of the headwater height (i.e., 85% submerged).

Calculations of this case were carried to $t=15$ s, at which time the headwater flow rate was varying by about 0.8% during the last couple of seconds, and the pressure at the H_a location was varying by less than 1%. At location H_b there remains a larger variation in pressure because of small disturbances in the fluid downstream of the location where the surface undergoes a jump in elevation.

Even though the flow is submerged, the *FLOW-3D* results are very regular and smooth looking. No computational difficulties were experienced in obtaining these results. Sample plots from the computation are contained in Fig. 5. The vertical plane of symmetry is shown in Fig. 5 (top), with a closer view of the submerged region shown in Fig. 5 (bottom).

The fluid exhibits a small jump in elevation just downstream of the flume's throat. A relatively slow flow velocity exists in the top layer of fluid following the jump. In real cases this region consists of a turbulent hydraulic jump containing some reversed flow, but we do not see this (probably because of limited numerical resolution and because of the LES turbulence model used in the computations).

The surface jump is a step in height about equal to one computational mesh cell. Because our model is formulated in terms of the conservation of mass and momentum, we expect flow rates and transition heights to be correct, even if we don't predict all the micro-details of the transition region.

The computed flow rate in this submerged case is 2.56 cfs, which is 94% of the computed flow rate under free-discharge conditions. This value might be reduced slightly if we were to continue the calculations to later times. The fact that the flow rate has been reduced below the free discharge value is indication that submerged conditions exist.

Reference WMM gives the expected flow rate under submerged conditions (see Fig. 28 of WMM) in terms of the static pressure at location H_b , but this is not readily available in our computations. Instead, we use the tailwater head of 0.68 feet, which should be nearly equivalent to H_b . This value gives an 85% submergence, and according to WMM the flow rate at this submergence should be reduced by 0.42 cfs to 2.43 cfs, or 85% of the free discharge value. Our computed value is larger than the empirical value by 0.13 cfs or 5.3%.

Alternatively, if we use the more recent data in the memorandum by H. Peck mentioned earlier, the 85% submerged flow rate would be 2.575 cfs, in which case our computed rate is only 0.6% low. Furthermore, the Peck data predicts the flow will be 92% of the free discharge rate at 85% submergence, while our computations give 94%. These comparisons are remarkably good.

HIGHLY SUBMERGED PARSHALL FLUME

Our last example is for 95% submergence, which is achieved by raising the tailwater height to 0.76 feet. For this example, we lowered the top of the grid slightly and increased the vertical resolution in the vicinity of the free surface because surface variations were expected to remain small. The minimum cell size in the free surface region was 0.02 feet, but this is only one half of the difference between the headwater and tailwater heights. Clearly, we still have severely limited resolution of the surface behavior in this example. Even so, the computations produce quite good results, which is an indication of the robustness and underlying soundness of the *FLOW-3D* formulation.

The calculation was carried to 40 s, which required about 8.17 hours of CPU time. All monitored quantities such as flow rates and pressures appeared to be leveling off to quasi-steady values by about 30 s. However, they continue to show small periodic oscillations about steady mean levels. For example, the headwater flow rate has a 1% peak-to-peak oscillation amplitude. There is some indication that these oscillations may be slowly damping out.

The late-time oscillations appear to have a period close to the transit time for waves to travel from the flume throat to the outflow boundary and return. It is not certain, however, if this is really the origin of the oscillations.

Figure 6 contains the full midplane and closeup plots for this case at the end of the computation. Average headwater and tailwater flow rates are nearly equal at 1.84 cfs. This is above the WMM table value by 0.24 cfs (13%) and above the Peck correlation by 0.37 cfs (27%). As observed by Peck, however, the determination of flow rates above 86% submergence is difficult, and large errors may exist in measured values as well as in the correlations. In any case, our computed flow rate is 67% of the computed free discharge value, confirming the rapid drop in flow rate at high submergence levels.

DISCUSSION

We have not attempted to directly study the bifurcated flow conditions observed by H. Peck (see previous reference) when the submergence is in the 90% range. Observations of this region in the Bureau of Reclamation one foot flume suggest that the flow entering the throat can have two marginally stable states and will jump between these states in a random fashion. This type of behavior is characteristic of a flow instability and may not be possible to model in detail because of its chaotic aspects.

The jump in surface height downstream of the throat entrance is almost always going to be turbulent. Flow in this region is characterized by fast moving fluid coming through the throat and passing under slower moving fluid on the surface that is trying to move upstream at the insistence of the tailwater head. The boundary of the two fluid layers is a shear layer that readily degenerates into turbulent eddies.

Hydraulic jump transitions are described by the conservation of mean momentum and mass. The mean kinetic energy across a jump is not conserved and some mechanism must exist to dissipate this excess kinetic energy. Usually this mechanism is turbulence, i.e., more or less random eddies develop that eventually dissipate into heat and sound.

In the numerical model we have tried to represent turbulence by a localized increase in viscosity, where the increase is proportional to the local shear magnitude. If the turbulent viscosity is large enough to dissipate the excess mean kinetic energy in the jump, turbulence will not develop in the form of explicitly computed eddies or regions of reverse flow. Nevertheless, the jump transitions and mean flow characteristics will still be correct.

SUMMARY

To summarize, we have shown that *FLOW-3D* can easily compute both free discharge and submerged flow conditions in Parshall flumes. The computed results agree very well with published flow rates and do not require excessive amounts of computation time or access to super computers.

Many useful and interesting studies extending these results would be easy to perform. For instance, one could study the influence of inlet conditions (e.g., asymmetries, obstructions, etc.) or the effects of settlement (e.g., tilt the flume by changing the direction of gravity) or the influence of shape and size changes in different portions of the flume (e.g., adding a venturi section). None of these studies would be difficult to implement in *FLOW-3D*.

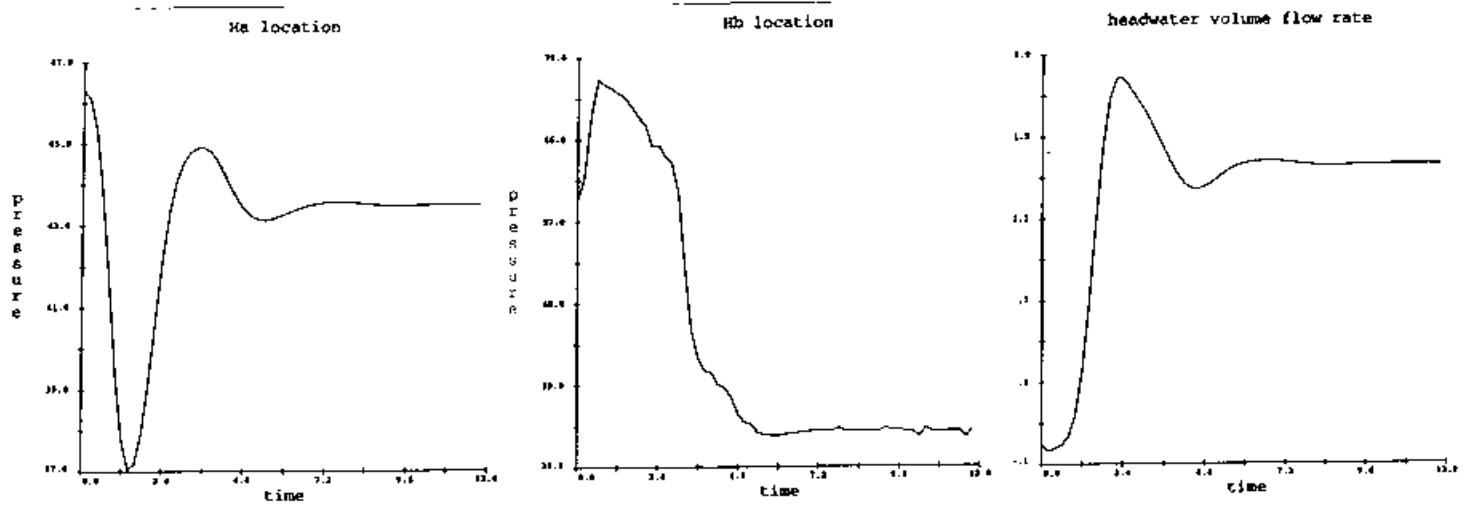


Figure 3. Free discharge pressure histories H_a (left) and H_b (middle). Headwater flow rate history (right).

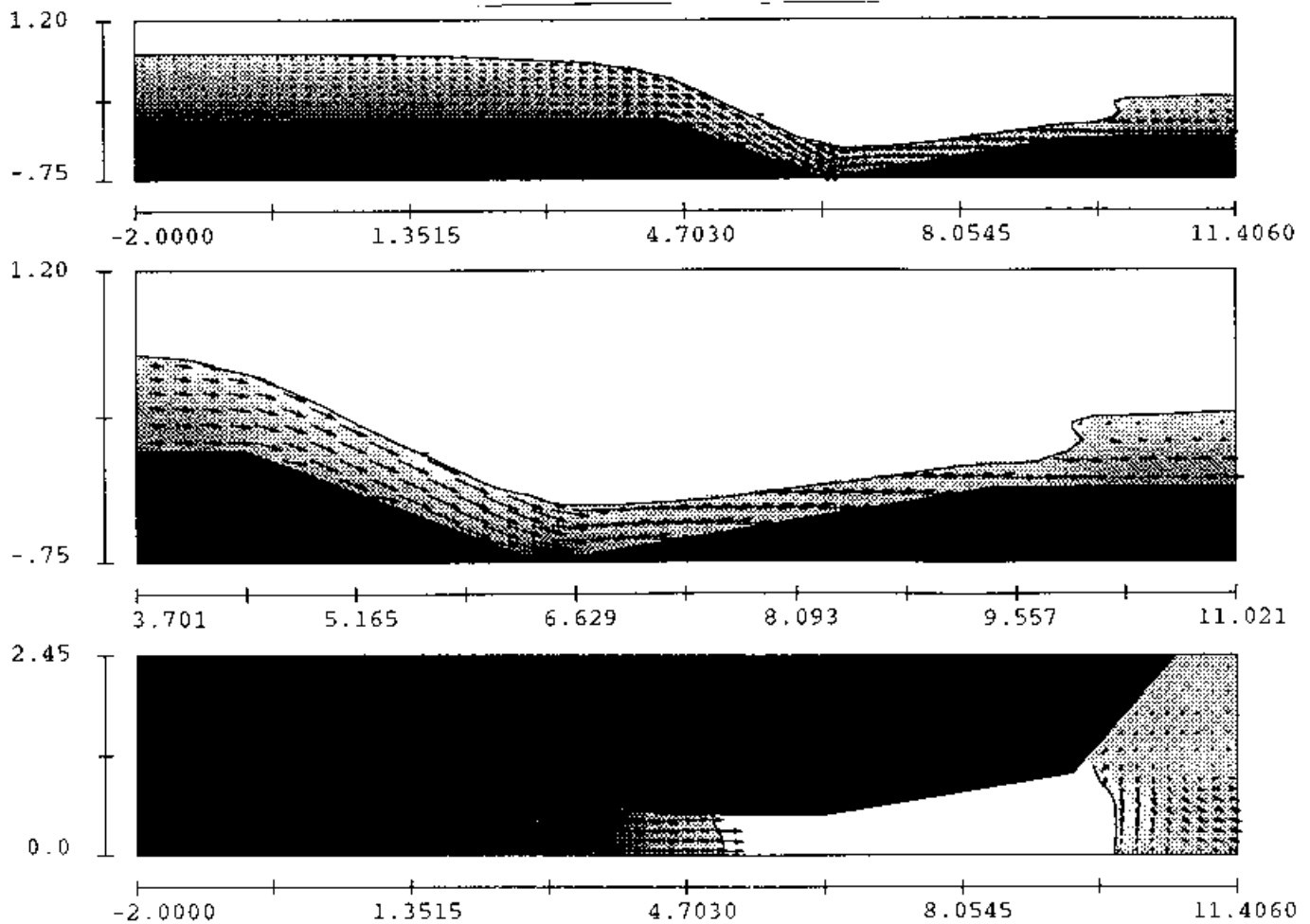


Figure 4. Free discharge results: vertical symmetry plane (top), throat region (middle) and horizontal slice (bottom).

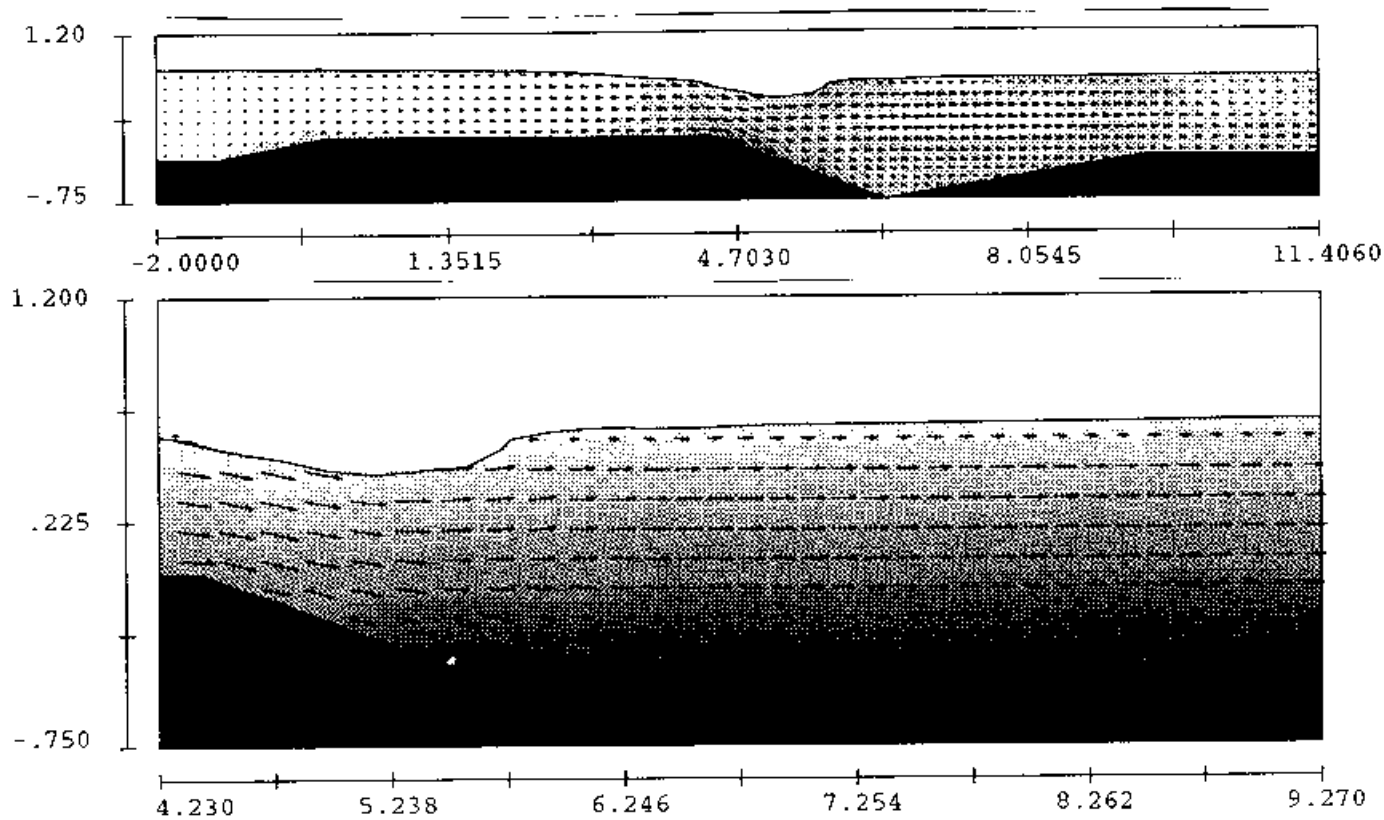


Figure 5. Results with 85% submergence: vertical symmetry plane (top) and throat region (bottom).

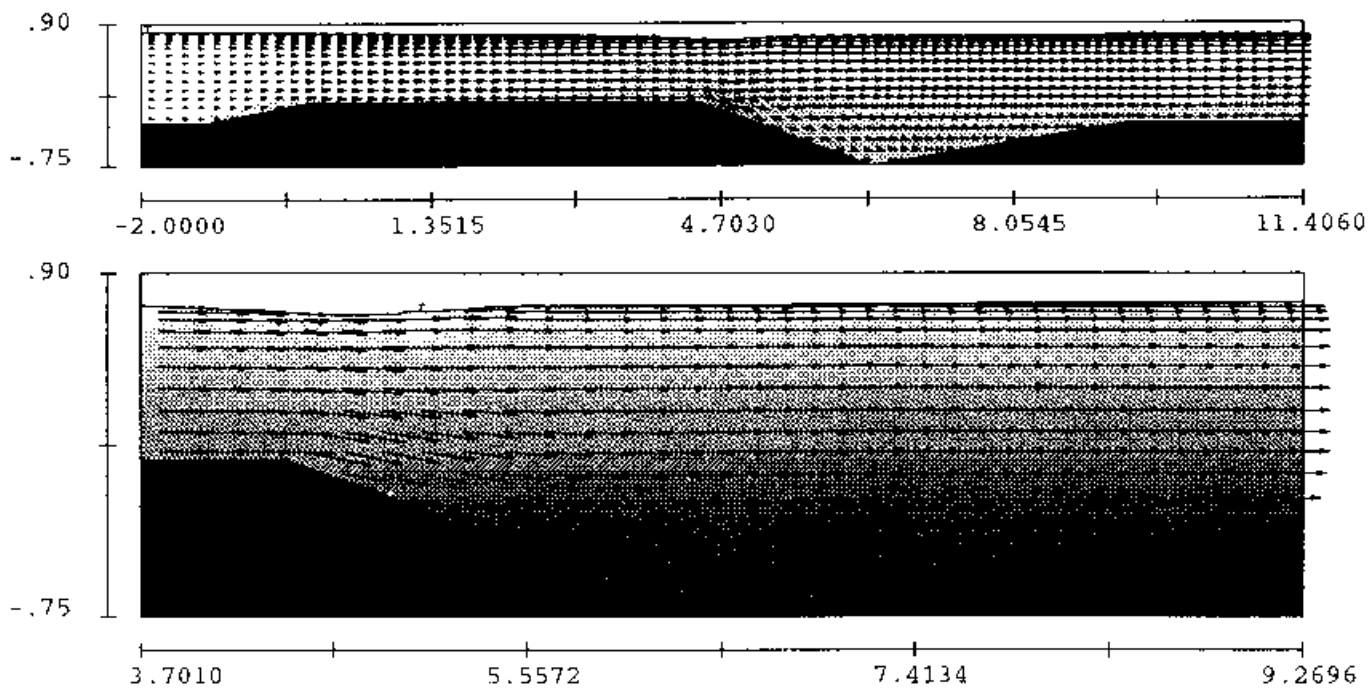


Figure 6. Results with 95% submergence: vertical symmetry plane (top) and throat region (bottom).